Decoherence induced by anisotropic hyperfine interaction in Si spin qubits

W. M. Witzel,[1] Xuedong Hu,[2] and S. Das Sarma[1]

[1]*Condensed Matter Theory Center, Department of Physics, University of Maryland, College Park, Maryland 20742-4111, USA*
[2]*Department of Physics, University at Buffalo, SUNY, Buffalo, New York 14260-1500, USA*
(Received 2 May 2007; revised manuscript received 14 June 2007; published 31 July 2007)

We study Si:P donor electron spin decoherence due to anisotropic hyperfine (AHF) interaction with the surrounding nuclear spin bath. In particular, we clarify the electron spin echo envelope modulation (ESEEM) in the Si:P system and the resonancelike contributions from nuclear spins in various shells away from the P atoms. We suggest an approach to minimize AHF-induced decoherence by avoiding the resonances and orienting an applied magnetic field along directions that can periodically eliminate contributions from the dominant nearest neighbor atoms. Our remarkable agreement with experiment demonstrates nearly complete understanding of electron spin decoherence in Si:P when combining ESEEM, spectral diffusion, instantaneous diffusion, and spin-lattice relaxation.

I. INTRODUCTION

The prospect of scalable solid state quantum information processing has created extensive interest in the study of coherent manipulation of single electron spins confined in semiconductor quantum dots or donor states. The clarification of single electron spin properties such as decoherence and quantum control should also be valuable scientifically in the field of nanostructure physics and very useful technologically in the context of spintronics and spin quantum memory.

Among the many semiconductor host materials, silicon is particularly enticing[1] due to its deep-rooted connection to the modern microelectronics industry. Furthermore, Si provides a remarkably quiet environment for electron[2,3] and nuclear[4] spin qubits since ^{28}Si, its most abundant isotope, has no net nuclear spin, and spin-orbit interaction is weak in Si. In this context, Si, with P donor electron spins as qubits, is an ideal semiconductor material for quantum information processing. The donor electron spin dephasing time T_2 as measured directly (and calculated theoretically) by spin echo decay is extremely long (many milliseconds in contrast to microseconds in GaAs) and can be further enhanced via isotopic purification. However, a strong anisotropic hyperfine (AHF) interaction in Si presents a formidable challenge for Si spin quantum computation; it produces finite spin dephasing relatively quickly that cannot be eliminated by spin refocusing techniques, and could potentially nullify the advantage of long spin T_2 time in Si.

This paper details the effects of the AHF interaction on donor electron spin qubits in Si:P. We discuss this interaction and present our Hamiltonian formalism in Sec. II. In Secs. III and IV, we formulate the problem of electron spin evolution and decoherence due to the AHF interaction in the context of free induction decay and (Hahn) spin echoes, respectively. We compare theoretical computations with experimentally observed spin echo envelopes in Sec. V, where we demonstrate nearly complete theoretical understanding of the decoherence of the Si:P electron spin qubit. Combining AHF-induced electron spin echo envelope modulation (ESEEM) with decoherence from spectral diffusion, instantaneous diffusion, and spin-lattice relaxation, we account for all major sources of decoherence and achieve nearly perfect quantitative agreement with Hahn echo decay experiments. We believe that AHF interaction supplies the final piece of the puzzle with respect to understanding Si:P electron spin decoherence. Furthermore, Sec. VI provides valuable insight into AHF-induced decoherence and a prescription for its suppression. Without proper treatment, this decoherence can violate the stringent fault-tolerant requirements of qubit fidelity much sooner than the nominal T_2 time suggests. While there are *no* existing spin echo techniques to generally remove AHF-induced echo modulations,[5] we suggest a concrete method for suppressing this decoherence and clarify requirements on the applied magnetic field for spin quantum computation in Si. We give concluding remarks in Sec. VII.

II. ANISOTROPIC HYPERFINE INTERACTION

The hyperfine (HF) interaction between an electron and a nuclear spin describes the magnetic dipolar coupling between the two spin species.[6] With $\hat{\mathbf{S}}$ denoting the spin operator of the electron and $\hat{\mathbf{I}}$ that of the nucleus, the HF Hamiltonian is given by $\hat{\mathcal{H}}_{HF} = \hat{\boldsymbol{I}} \cdot \boldsymbol{A} \cdot \hat{\boldsymbol{S}}$, where the hyperfine tensor $\boldsymbol{A}$ is given by

$$A_{ij} = \gamma_I \gamma_S \hbar^2 \left(\frac{8\pi}{3} |\Psi(\mathbf{0})|^2 \delta_{ij} + \left\langle \Psi \left| \frac{3 x_i x_j - \boldsymbol{r}^2 \delta_{ij}}{\boldsymbol{r}^5} \right| \Psi \right\rangle \right), \tag{1}$$

with the electron position measured relative to the site of the nucleus, Ψ the electron wave function, and γ_S and γ_I the gyromagnetic ratios of the electron and the nucleus. The first term of Eq. (1) is the *isotropic* Fermi contact HF interaction. The second term is *anisotropic*. Which part of the interaction is more important depends on the electron wave function. For example, the GaAs conduction band minimum occurs at the Γ point of the Brillouin zone, where the electron Bloch function is mostly atomic *s* type, so that HF interaction in GaAs between an electron near the conduction band minimum and the surrounding nuclear spins is essentially isotropic. On the other hand, the degenerate conduction band mini-

mum for Si occurs close to the X point of the Brillouin zone, where the electron Bloch functions have significant contributions from p and d atomic orbitals,[7–9] so that HF interaction between an electron near the conduction band minimum, such as an electron confined to a donor or a quantum dot, and the surrounding nuclear spins has strong anisotropic characteristics. Indeed, AHF interaction has been studied extensively in the Si:P system in the 1960s and 1970s.[7,10,11] The strength of AHF has been accurately measured[11] and calculated[7] for the phosphorus donor electron. In the context of solid state spin quantum computation, however, much of the existing literature only take into account the contact HF [first term in Eq. (1)] in considering electron spin decoherence.

To analyze how AHF leads to spin decoherence, we consider a single P donor in Si, with the donor-bound electron interacting with the P and randomly distributed ^{29}Si nuclear spins. We assume the limit of a strong magnetic field (>100 mT is sufficient) applied in the z direction such that electron spin flips are suppressed due to its large Zeeman energy. Since $\gamma_S \gg \gamma_I$, it is appropriate to take the limit where $\hat{S}_z$ is conserved but not $\hat{I}_z$ (of any nucleus). In this limit, we write the Hamiltonian (in $\hbar = 1$ unit) as $\hat{\mathcal{H}} = \hat{\mathcal{H}}_0 + \Sigma_n \hat{\mathcal{H}}_n$ with

$$\hat{\mathcal{H}}_0 = \omega_S \hat{S}_z + A_P \hat{S}_z \hat{I}_z^P - \omega_P \hat{I}_z^P, \tag{2}$$

$$\hat{\mathcal{H}}_n = A_n \hat{S}_z \hat{I}_{nz} + B_n \hat{S}_z \hat{I}_{nx'} - \omega_I \hat{I}_{nz}. \tag{3}$$

We separate the Hamiltonian into $\hat{\mathcal{H}}_0$, involving the electron Zeeman energy and the donor nucleus, and $\hat{\mathcal{H}}_n$, involving the nth ^{29}Si nucleus in the surrounding lattice (other Si isotopes have zero spin). In our notation, $\hat{\boldsymbol{S}}$, $\hat{\boldsymbol{I}}^P$, and $\hat{\boldsymbol{I}}_n$ denote spin operators of the electron, P nucleus, and the nth ^{29}Si nucleus, respectively. $\hat{I}_{nx'}$ gives the nuclear spin operator in an x'-axis orientation so that there is no $\hat{S}_z \hat{I}_{ny'}$ contribution (thus we generally have a different x' orientation for each n). Given an applied magnetic field strength of B, we define $\omega_\square = \gamma_\square B$ as the Zeeman frequency for the electron, P nucleus, or a ^{29}Si nucleus with $\square = S, P$, or I, respectively. A_P denotes the HF coupling between the electron and the P nucleus. Both contact HF and the $\hat{S}_z \hat{I}_z$ part of the AHF interaction are contained in A_n. The remaining AHF interaction in our strong field limit is contained in B_n and gives the relevant anisotropy, mixing different directional components of $\hat{\boldsymbol{S}}$ and $\hat{\boldsymbol{I}}$.

Qualitatively, due to the anisotropic term $B_n \hat{S}_z \hat{I}_{nx'}$ in $\hat{\mathcal{H}}_n$, the quantization axis for the precession of the ^{29}Si nuclear spin is dependent on the state of the electron spin. Conversely, the electron spin is affected by the precession of the nuclear spin. The resulting electron spin free induction decay (FID) in Si:P has been explored in Ref. 12 and will be briefly reviewed in Sec. III. It is shown[12] that the donor electron spin could lose more than 1% of its coherence after *only* about 10 μs if a ^{29}Si atom is in one of the nearest neighbor (E shell) sites. This would be disastrous for quantum computation where the error rate must stay below typical fault tolerance requirements of 10^{-6}–10^{-4}. Fortunately, as we will show in Sec. VI, AHF-induced decoherence may be drasti-

cally suppressed by applying precisely timed pulses and a sufficiently strong magnetic field along special directions of high symmetry.

III. EFFECT OF ANISOTROPIC HYPERFINE ON FREE INDUCTION DECAY

$\hat{\mathcal{H}}_n$ of Eq. (3) for different n commute with each other so that the free evolution operator, in the interaction picture, becomes the product of evolution operators for each n:

$$\hat{U}_0(t) = e^{-i\hat{\mathcal{H}}t} = e^{-i\hat{\mathcal{H}}_0 t} \prod_n e^{-i\hat{\mathcal{H}}_n t}. \tag{4}$$

We may write this evolution operator in the form

$$\hat{U}_0(t) = \hat{U}_0^+(t)\hat{P}_\uparrow + \hat{U}_0^-(t)\hat{P}_\downarrow, \tag{5}$$

where $\hat{P}_\uparrow = |\uparrow\rangle\langle\uparrow|$ and $\hat{P}_\downarrow = |\downarrow\rangle\langle\downarrow|$ are up and down projection operators for the electron spin. In other words, $\hat{U}_0^\pm(t)$ denotes the free evolution of the nuclei given an electron spin that is either up or down. The free evolution operator may take the form of Eq. (5) because the Hamiltonian only involves $\hat{S}_z$ and no other electron spin operator. For the same reason, only dephasing occurs for the electron spin and thus only the off-diagonal elements of the electron spin's density matrix may evolve. Assuming unpolarized (random) nuclei, after time t the off-diagonal element of the electron spin's density matrix becomes[12]

$$\frac{\langle\downarrow|\rho(t)|\uparrow\rangle}{\langle\downarrow|\rho(0)|\uparrow\rangle} = \prod_n \left\{ a_n^2 \cos\left(\frac{\Delta\omega_n}{2}t\right) + b_n^2 \cos(\bar{\omega}_n t) \right\}, \tag{6}$$

where $\Delta\omega_n = \omega_{n+} - \omega_{n-}$, $\bar{\omega}_n = (\omega_{n+} + \omega_{n-})/2$, with

$$\omega_{n\pm} = \sqrt{\left(\pm\frac{A_n}{2} - \omega_I\right)^2 + \left(\frac{B_n}{2}\right)^2}, \tag{7}$$

and $a_n^2 + b_n^2 = 1$ (details in Ref. 12). $\omega_{n\pm}$ are precession frequencies for nucleus n. Nucleus n will precess at a frequency of ω_{n+} or ω_{n-} given an up or down electron spin, respectively. In general, if the electron spin is in a superposition of up and down states, the nuclear spin dynamics will contain both these frequencies. As mentioned before, numerical evaluation of Eq. (6) shows[12] that the donor electron spin could lose more than 1% of its coherence in ~10 μs if a ^{29}Si atom is in one of the nearest neighbor (E shell) sites.

IV. ELECTRON SPIN ECHO ENVELOPE MODULATIONS

The key question now is whether the AHF-induced electron spin decoherence can be suppressed. It is well known that spin echo techniques such as Hahn echo can be used to remove dephasing caused by the spatial variation of local magnetic fields (the inhomogeneous broadening). However, the AHF-induced FID is a dynamical effect and, as such, cannot be removed by Hahn echo. Instead, AHF causes the echo envelope to oscillate, which is known within the electron spin resonance community as ESEEM.[6,13,14] This effect is particularly useful in chemistry for the identification of

nuclear spin species of molecular sites.[6,14] The focus of the present study is to investigate ESEEM in the Si:P system[15–18] and explore possible ways to reduce the decoherence effect of AHF interaction with ^{29}Si in the context of spin quantum computation.

In the Hahn echo sequence, after initializing the electron spin (which is necessary for experimental decoherence measurements, but is neither applicable to qubit preservation nor necessary in the current discussion), the system evolves freely for a time τ, then a resonant pulse rotates the spin by π about an axis perpendicular to the magnetic field, and then an echo is observed after another τ in time (for shorthand, we use $\tau \to \pi \to \tau$ to denote this sequence). For convenience in our formalism, though it makes no difference, we apply a second π pulse in order to bring the spin back to its original orientation (apart from decoherence): $\tau \to \pi \to \tau \to \pi$. Assuming an ideal applied π pulse and free evolution in the diagonal form of Eq. (5), the evolution over the echo sequence has the diagonal form

$$\hat{U}_{\text{Hahn}} = \hat{U}^+_{\text{Hahn}} \hat{P}_\uparrow + \hat{U}^-_{\text{Hahn}} \hat{P}_\downarrow, \qquad (8)$$

$$\hat{U}^\pm_{\text{Hahn}} = \hat{U}^\mp_0(\tau) \hat{U}^\pm_0(\tau). \qquad (9)$$

Mathematically, spin echo is the magnitude of the expectation value of the electron spin (a measure of the fidelity of the qubit) after the quantum system evolves according to the echo sequence [Eq. (8)]. As is physically measured, the echo is the average spin of an ensemble of electron spins that undergo the Hahn echo evolution. Assuming only $\hat{S}_z$ electron spin interactions, as we do, maximum decoherence occurs for an electron that is initially perpendicular to the z direction (the direction of the applied magnetic field), and the spin echo is more precisely defined with such an initial electron spin state. In the experimental measurement, the ensemble of electron spins are initialized to point in the same direction perpendicular to this axis. Where $\langle \cdots \rangle$ is the quantum mechanical average over initial bath states, this Hahn echo envelope may be expressed as[19]

$$V(\tau) = \langle [\hat{U}^-_{\text{Hahn}}]^\dagger \hat{U}^+_{\text{Hahn}} \rangle. \qquad (10)$$

In computing the expectation value, we average over all initial nuclear states, assuming a completely disordered and unpolarized initial bath as in Sec. III.

Electron spin echo decays as a function of τ due to internuclear interactions. In the current study, we do not focus on this process, known as spectral diffusion, which has been studied by two of us[19] previously. On top of this decay, AHF coupling [Eq. (3)] produces envelope modulations or ESEEM.[6,14] Neglecting the internuclear interactions, the ESEEM due to each nucleus factors into the Hahn echo evolution separately [Eq. (4)]. Given that only a fraction f of the Si nuclei have nonzero spin (^{29}Si), we have the following ESEEM amplitude averaged with respect to isotope configurations:[13,20]

$$V(\tau) = \prod_n [(1 - f) + f V_n(\tau)], \qquad (11)$$

$$V_n(\tau) = 1 - \frac{k_n}{2} [1 - \cos(\omega_{n+}\tau)][1 - \cos(\omega_{n-}\tau)], \qquad (12)$$

$$k_n = (\omega_I B_n)^2 / (\omega_{n+}\omega_{n-})^2, \qquad (13)$$

where $\omega_{n\pm}$ are nuclear precessional frequencies defined by Eq. (7). In the literature, k_n is called the modulation depth parameter.[20] The maximum modulation (deviation from 1) of $V_n(\tau)$ is $2k_n$, so that k_n is a measure of modulation amplitude. In the "worst-case" scenario, when modulations from all nuclei combine constructively, the maximum possible modulation depth averaged over isotopic configurations is given by

$$\text{Max}[1 - V(\tau)] = 1 - \prod_n [1 - 2f k_n]. \qquad (14)$$

In Fig. 1(a), we show this maximum modulation as a function of field strength due to various nuclear shells (symmetry-related sets of lattice sites[7]). We use experimentally determined contact and AHF coupling constants for 22 nuclear shells (which include about 150 symmetry-related nuclear sites) taken from Refs. 7 and 11.

V. UNDERSTANDING EXPERIMENTAL OBSERVATION OF SPIN ECHO DECAY AND MODULATION

The Hahn echo decay of Si:P donor electron spin has been studied in several recent experiments.[15–18] A previous quantum theory of nuclear-induced spectral diffusion (SD) by two of us[19] shows very good quantitative and qualitative agreement with these experimentally determined decay curves. However, the agreement is not perfect, especially at short times, because we previously neglected the effects of AHF interactions that produce modulations of the echo envelope, i.e., ESEEM. We now add this last piece to the puzzle to achieve truly remarkable agreement with experimental echo decay curves and thus demonstrate a nearly complete understanding of Si:P donor electron spin decoherence.

Figure 2(c) shows excellent agreement of our ESEEM calculations with experimental data reported in Ref. 16. The theory calculations do use five separate fitting parameters: normalization, strain distribution width, relaxation time, SD time, and a SD exponent. The first three of these parameters (described momentarily) may be fixed for all different directions of the applied magnetic field. Thus, in Fig. 3, which shows comparison with experiment[16] for ten different magnetic field directions, we use only two fitting parameters per curve. These two fitting parameters characterize the SD decay and are compared with the results of our SD theory[19] in Fig. 4. Considering that we use, in our SD analysis, the Kohn-Luttinger envelope function within the effective mass approximation for the donor electron,[21] which is known to be less reliable near the phosphorus atom,[22,23] the agreement is quite good. There appears to be, however, some discrepancy between the fit and the theory for the SD exponent when the applied field is close along the [001] lattice direction: theory expects $n = 2.3$ and the fit yields $n = 2.5$. It is probably not coincidental that the nearest neighbor dipolar coupling vanishes when the applied field points along the [001] direction. Perhaps we have overlooked some interactions that become
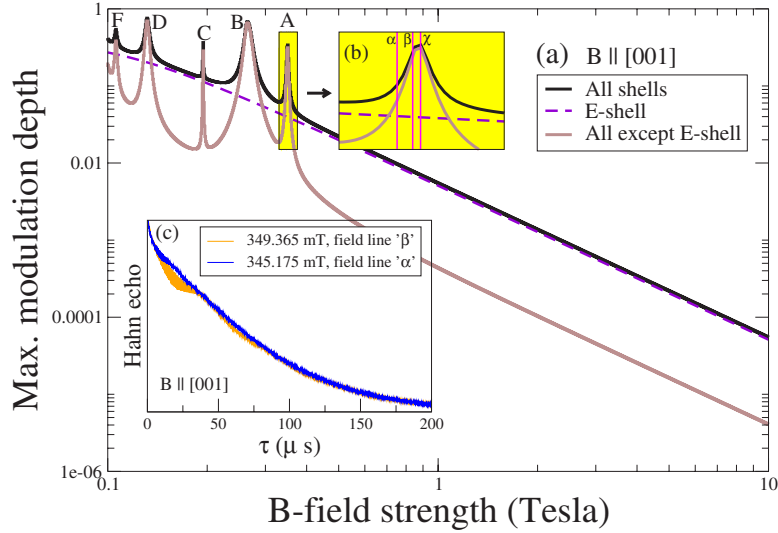
FIG. 1. (Color online) (a) Maximum modulation depth [Eq. (14)] in natural Si averaged over isotopic configurations with an applied magnetic field B parallel to the [001] lattice direction considering all shells (provided in Ref. 7), just E-shell sites (nearest neighbors of the P donor), and all shells except the E shell. This maximum depth gives the worst-case scenario of constructively interfering nuclear ESEEM contributions and is useful for identifying the major sources of modulations. When one shell of nuclei dominate, the worst-case maximum modulation depth is close to the actual observed modulation depth. Near the cancellation condition, $\omega_I \sim A_n/2$, for each shell of nuclei is a peak labeled by the shell letter where that shell dominates; away from these peaks, the E shell is seen to dominate. (b) Enlargement of the A shell peak marking three field strengths, α, β, and χ, used by experiments presented in this paper. (c) Corresponding experimental (Ref. 5) Hahn echo decay at field strengths α and β for the same Si:P sample. Relatively high doping, 10^{16} P/cm^3, results in fast exponential relaxation due to instantaneous diffusion, but ESEEM is still observed.

important when the dipolar interaction is weak. Overall, however, we do demonstrate good theoretical understanding of Si:P electron spin decoherence in Figs. 2–4.

We now describe the fitting parameters in more detail. The AHF-induced ESEEM [Eq. (11)] for a single electron spin, using the experimentally determined coupling constants for 22 nuclear shells from Ref. 7, is shown in Fig. 2(a). Random defects such as dislocations cause strain effects (such as electron population shifts between different Si valleys) that slightly alter the coupling constants for different donors. Strain effects result in narrow distributions for the values of HF coupling constants and/or Zeeman frequencies and effectively dampen the ESEEM signal for an ensemble of spins. This is shown in Fig. 2(b) where, in order to fit the experimental results, we assume a Gaussian distribution for HF frequencies with a 0.4% width.[24] We believe strain is the culprit of this distribution of HF interaction strengths because of two reasons. First, experimentalists observe strain effects orders of magnitude larger than this when applying a small stress on their sample, so it is quite plausible and likely that random defects are generating the strain, consistent with our excellent fit.[5,25,26] Second, other neglected interactions, such as electrons interacting with nuclei at different donors and dipolar interaction between nuclear spins, are much too small to account for this effect. If we do not assume a distribution of HF coupling constants, the echo modulation would continue with a constant amplitude [see Eq. (12)] until eventually nuclear spin relaxation kicks in. This is obviously not what is observed experimentally.[15–18]

In addition to strain, Fig. 2(b) shows the stroboscopic effect that emerges when we sample the same values of τ as those reported in the experiment. The theoretical (orange)
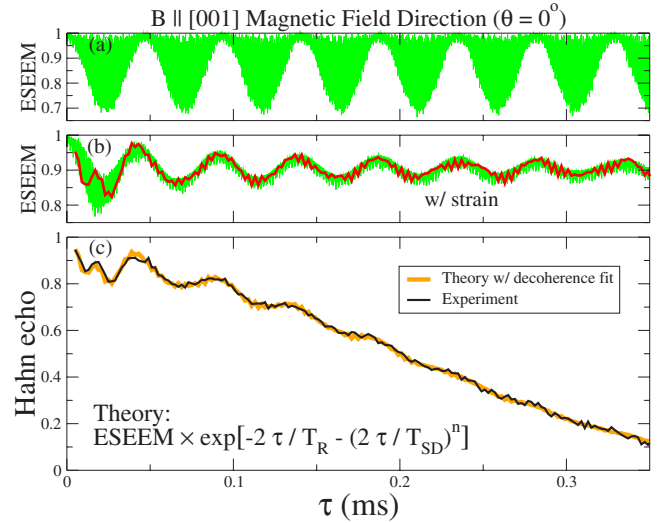

FIG. 2. (Color online) AHF-induced ESEEM in Si:P with an applied magnetic field in the [001] direction. (a) Pure AHF-induced ESEEM for a single electron spin. The green "blob" is one curve with high frequency components. (b) Before matching the ESEEM to experiment, we must account for strain effects in the ensemble of donor electrons (green); we must additionally sample at the same values of τ as the experiment (red) yielding a stroboscopic effect. (c) Comparison with experiment (black). In our calculation, we combine decoherence effects of ESEEM, (non-Markovian) nuclear-induced SD, and (Markovian) exponential relaxation by simply multiplying them together. The orange curve gives ESEEM of our theory [red curve in (b)] multiplied by $\exp[-2\tau/T_R]\exp[-(2\tau/T_{SD})^n]$, where T_R, T_{SD}, and n are fitting parameters for the relaxation time, SD time, and SD exponent, respectively.
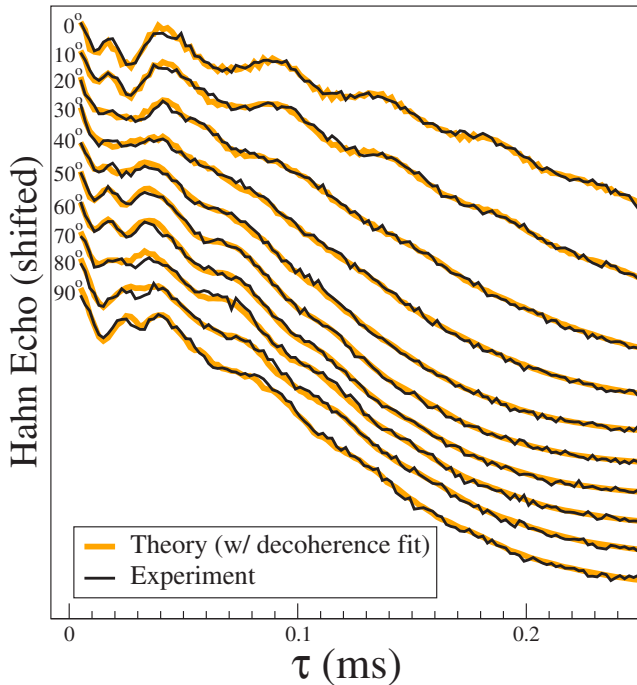
FIG. 3. (Color online) AHF-induced ESEEM in Si:P for ten different curves corresponding to ten different magnetic field angles ranging from the [001] to the [110] directions. The plots are shifted in order to distinguish each angle. All fits use the same normalization, strain distribution width (0.4%), and relaxation time ($T_R=2.17\pm0.02$ ms) parameters. There are two fitting parameters per curve: the SD time, T_{SD}, and the SD exponent, n. These fitting parameters are compared with our SD theory (Ref. 19) in Fig. 4.

curve in Fig. 2(c) shows the ESEEM result of Fig. 2(b) multiplied by $\exp[-2\tau/T_R]\exp[-(2\tau/T_{SD})^n]$ to account for independent effects of Markovian relaxation and non-Markovian nuclear-induced SD. After we normalize the signal strength
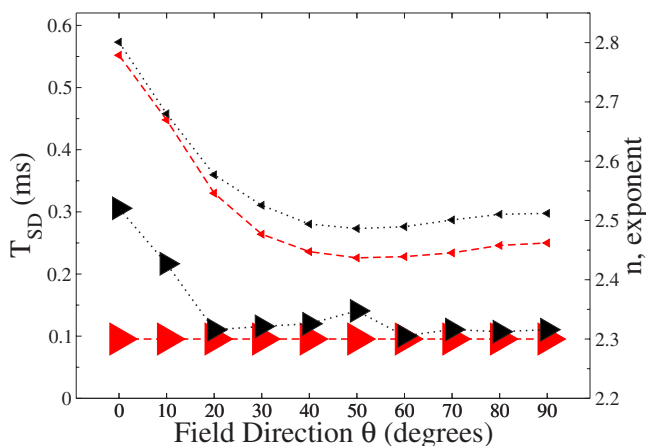

FIG. 4. (Color online) Comparison between the SD fitting parameters (black triangles connected with dotted lines) of Fig. 3 and the theoretical predictions (red triangles connected with dashed lines) of our SD (Ref. 19) theory. Right (left) triangles correspond to n (T_{SD}); sizes approximate fitting uncertainty. The experimental n fit deviates from theory (2.30 ± 0.05) only at small angles, where nearest neighbor dipolar flip-flop interactions approach zero.

as an additional fit (the experiment only gives the Hahn echo decay on a relative scale based on the strength of the observed signal), we obtain excellent agreement with the experimental results [black curve in Fig. 2(c)]. Again, we use a total of five fitting parameters in Fig. 2; however, we use only two fitting parameters per curve in Fig. 3 and these two SD parameters are compared with theoretical results via Ref. 19 in Fig. 4.

Although nuclear-induced SD and ESEEM both result from interactions with the nuclear spin bath, we have confirmed that it is appropriate to treat them independently. Nuclear-induced SD results from very small contributions from many thousands of pairs of flip-flopping nuclei.[19] The weak nuclear dipolar coupling that is responsible for SD is too small to have any significant impact on the ESEEM-contributing nuclei that have a much stronger HF coupling to the electron. To be rigorous, we have made explicit cluster expansion calculations[19] that include the AHF interaction. ESEEM emerges from one-cluster contributions, and the two-cluster contributions are negligibly changed with the introduction of AHF coupling. This calculation confirms the independence of these two decoherence channels.

The Markovian relaxation is dominated by instantaneous diffusion (ID) that results from interactions between the resonant electron spin donors.[6] Having a concentration of 8×10^{14} donors/cm^3 in these experiments,[16] with half of those at resonance with the applied pulses (determined by whether the P donor nucleus has an up or down spin), yields an ID time of $T_{ID}\approx3$ ms,[6] accounting for most of the $T_R\sim2.2$ ms relaxation. A further relaxation process with a decay time of about 8.3 ms would be needed to account for the remaining contribution to T_R (the inverse of the decay times are additive). With these experiments performed at 8 K,[16] this may be attributed to temperature-dependent spin-lattice relaxation; 8.3 ms is fairly consistent with reported 10–25 ms temperature-dependent relaxation time in Si:P at 8 K (a wide uncertainty range is due to strong temperature dependence and offsets in temperature calibration).[15]

It is important to emphasize here that the theoretical fitting for the echo modulations (separate from spectral diffusion and relaxation) uses experimentally obtained AHF interaction strength. The only variable fitting parameter for echo modulations is the 0.4% distribution of the AHF interaction strength, which allows us to reproduce the decay of the echo modulation. In the meantime, as indicated in Fig. 4, the fit for spectral diffusion is an attempt to use a relatively simple functional form to represent our theoretical calculations in Ref. 19. Therefore the seemingly large number of fitting parameters involved here is not a blind attempt to obtain the best possible fit to the experimental measurements. Instead, they mostly provide a more transparent representation of a more sophisticated theory, and the remarkable agreement we obtain here illustrates that all the main decoherence mechanisms are represented, most likely, in our description.

VI. SUPPRESSING ANISOTROPIC-HYPERFINE-INDUCED ESEEM

After building confidence in our theoretical approach by comparing our results with experiments, we now address the
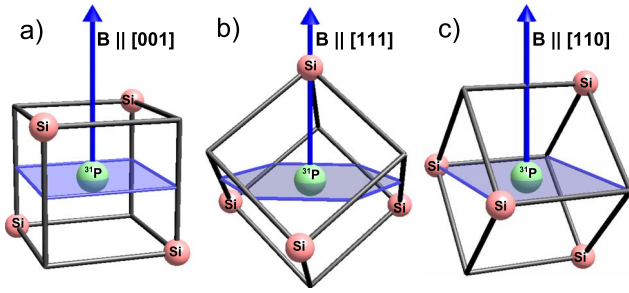
FIG. 5. (Color online) Special applied magnetic field directions that allow effective removal of echo modulation contributions due to E-shell nuclei (the four nearest neighbors to the P donor). The arrows and translucent sheets, respectively, indicate directions from the P atom parallel and perpendicular to the applied magnetic field. Sites in these direction give no anisotropic contribution ($B_n=0$) because these directions are, by symmetry, along the principal axes of the **A** tensor of Eq. (1); thus, the top site in (b) and the two in-plane sites in (c) do not contribute to ESEEM. In each of the three cases, the E-shell sites that *do* contribute are magnetically equivalent.

FIG. 6. (Color online) Echo modulations, $1-V(\tau)$, in natural Si with an applied field of 1 T in the [001] direction corresponding to Fig. 5(a). When sampling τ at multiples of $2\pi/\omega_+$ (or $2\pi/\omega_-$), the E-shell nuclei give no contribution to the echo modulations. Error bars, vertically asymmetric because of the logarithmic scale, correspond to the standard deviation resulting from random isotopic configurations; those with down arrows extend below the visible range.

question of how to suppress spin decoherence induced by AHF interaction. More specifically, we will show that this AHF-induced decoherence may be drastically reduced by carefully choosing the strength and direction of the applied magnetic field and by applying spin echo pulses with precisely prescribed timing.

One interesting and important feature of the maximum modulations shown in Fig. 1(a) is that a peak occurs when $\omega_I \sim A_n/2$ (with A_n positive) for each shell of atoms. At each such cancellation condition, as it is dubbed, the Zeeman and HF energies of nucleus n cancel when the electron spin is up but not down, freeing the nuclear spin from conservation of energy constraints conditional upon the state of the electron spin. Mathematically, ω_{n+} is minimized [Eq. (7)] so that k_n is at (or very near) its maximum, resulting in modulation depth peaks. This effect is shown experimentally by comparing the two echo decay curves in Fig. 1(c); the curve corresponding to a field strength closer to the center of the A-shell peak clearly exhibits stronger echo modulations. It turns out that the experiments discussed in Sec. V were performed with a magnetic field strength denoted as χ in Fig. 1(b), which is very close to the center of the A-shell peak, where echo modulations are particularly strong.

It is clear from this discussion that to minimize AHF-induced decoherence, cancellation conditions for all the shells with finite AHF coupling constant should be carefully avoided by properly selecting the applied magnetic field strength (or, in electron spin resonance, the corresponding microwave cavity frequency). Furthermore, away from the cancellation condition peaks, the E-shell nuclei (nearest neighbors to the P nucleus) have the strongest AHF coupling by far, so that they dominate the echo modulations by more than an order of magnitude, as seen in Fig. 1(a). Remarkably, the echo modulation due to these dominating E-shell nuclei can be effectively removed at special magnetic field orientations (Fig. 5) if we exploit the periodic restoration of electron spin coherence in the presence of nuclei that are seen by the electron as magnetically equivalent. This restoration arises
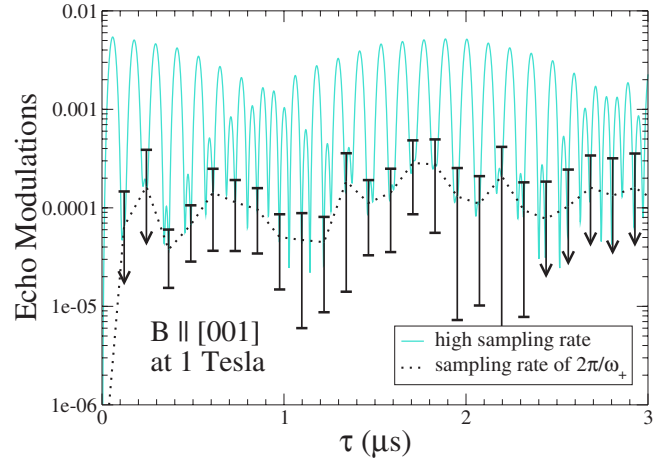
because $V_n(\tau)=1$ [Eq. (12)] when τ is a multiple of $2\pi/\omega_{n\pm}$ (either + or −). Note that such periodic restoration does *not* generally occur in the free induction case of Sec. III.

For special magnetic field orientations shown in Fig. 5, the contributing E-shell sites are magnetically equivalent with the same $\{\omega_{n-}, \omega_{n+}\}$; thus, the electron spin is periodically restored at the same values of τ regardless of isotopic (^{29}Si) configuration. In this way, E-shell contributions can effectively be eliminated as exemplified in Fig. 6. By orienting the magnetic field in one of the various special directions, the effects of all E-shell nuclei are simultaneously eliminated at periodic values of τ.

To understand the periodic restoration of ESEEM in the presence of magnetically equivalent nuclei, note that $\hat{U}_0^\pm(t)$ simply generates precession for each nucleus at a frequency of $\omega_{n\pm}$, respectively. For instance, given an electron spin that is up, the nuclear spin returns to its initial orientation after waiting for a time that is a multiple of $2\pi/\omega_+$. That is, assuming all nuclei being considered are magnetically equivalent, $\hat{U}_0^\pm(2\pi m/\omega_\pm)=1$ for any integer m. If we consider a Hahn echo sequence with $\tau=2\pi/\omega_+$, we have [see Eq. (9)] $\hat{U}_{\text{Hahn}}^\pm=\hat{U}_0^\mp(\tau)\hat{U}_0^\pm(\tau)=\hat{U}_0^-(\tau)$. Thus the evolution of the magnetically equivalent nuclei is independent of the electron spin, since $\hat{U}_{\text{Hahn}}^+=\hat{U}_{\text{Hahn}}^-$, so that the electron qubit is fully decoupled from these nuclei (apart from the effects of the neglected nuclei that are not magnetically equivalent to the others). This property is common to any balanced sequence in which an initially up or down electron (or the separate components of a superposition state) spends an equal amount of time being up and down. Specifically, we may apply our timing trick to eliminate E-shell modulations for the Carr-Purcell sequences[27,28] or concatenated dynamical decoupling sequences[29,30] that can be much more effective than the Hahn echo for mitigating other types of decoherence such as spectral diffusion.[28,30]

It is important to determine how sensitive our technique of suppressing AHF-induced decoherence is to errors in timing and magnetic field direction. Because the E-shell contributions oscillate at frequencies of ω_{n-} and ω_{n+}, the timing of the pulse sequence in order to remove this effect must be accurate with errors that are small compared with the period of these oscillations, $2\pi/\omega_{n-}$ and $2\pi/\omega_{n+}$. For magnetic fields that are $\gtrsim 1$ T, these oscillation frequencies [Eq. (7)] are dominated by the nuclear Zeeman frequency, $\omega_{n\pm} \approx \omega_I$, so that the periods are approximately $2\pi/\omega_I \sim 100$ ns, as is apparent in Fig. 6.

The timing is also affected by systematic uncertainty in either ω_{n+} or ω_{n-} (whichever we choose for synchronization) in a way that worsens in time and number of oscillation periods. The resulting uncertainty in time is given by

$$\delta\tau = \left(\frac{\delta\omega_{n\pm}}{\omega_{n\pm}}\right)\tau. \qquad (15)$$

Then, the requirement that $\delta\tau \ll 2\pi/\omega_{n\pm}$ yields the following restriction:

$$\tau \ll \frac{2\pi}{\delta\omega_{n\pm}}. \qquad (16)$$

When dealing with an ensemble, the uncertainty of $\omega_{n\pm}$ will be subject to strain effects. In Sec. V, we empirically determined strain effects causing a 0.4% distribution, which equates to a frequency uncertainty of about 10 kHZ. This implies that we are limited to $\tau \ll 100$ μs. On the other hand, the situation in a different experiment or sample could be quite different and would depend on the precise effects of strain on the E-shell nuclei, which is outside of the scope of this paper. Also, depending on the architecture of the proposed quantum computer, it may be possible to calibrate pulse timing to individual qubits rather than an ensemble, circumventing the uncertainty caused by strain.

Errors in the applied magnetic field direction *cannot* be fixed with calibration. If the magnetic field direction deviates from one of the three special directions in Fig. 5, the contributing E-shell nuclei will no longer be equivalent and nuclei that are supposed to be inert [e.g., the top nucleus in Fig. 5(b) and the two leftmost nuclei in Fig. 5(c)] will, in general, contribute to ESEEM. In order to address the question of sensitivity to the magnetic field direction, we first consider how angular uncertainty affects the uncertainty of $\omega_{n\pm}$:

$$\frac{\delta\omega_{n\pm}}{\delta\theta} = \frac{1}{\omega_{n\pm}}\left[\frac{\pm 1}{2}\left(\frac{\pm A_n}{2} - \omega_I\right)\frac{\delta A_n}{\delta\theta} + \frac{1}{4}B_n\frac{\delta B_n}{\delta\theta}\right].$$

We again assume that $\omega_{n\pm} \sim \omega_I$, so that

$$\max_n\left|\frac{\delta\omega_{n\pm}}{\delta\theta}\right| \approx \frac{1}{2}\max_n\left|\frac{\delta A_n}{\delta\theta}\right|. \qquad (17)$$

This is valid when $\max_n|A_n| \gtrsim \max_n|B_n|$, so that the δB_n contribution is negligible. We have verified this numerically by

calculating how A_n and B_n vary with respect to changing the magnetic field direction about an axis that rotates from [100] to [011]. Although we did not analyze full two-dimensional changes in direction, we do extract a characteristic scale of 50 kHz/deg for both $\delta A_n/\delta\theta$ and $\delta B_n/\delta\theta$ of the E-shell nuclei, which we expect to be general. In addition to $\omega_{n\pm}$, we must also consider how an error in the magnetic field direction away from [111] or [011] affects k_n for those nuclei which are not expected, ideally, to contribute. For such nuclei,

$$k_n \approx \left.\frac{1}{2}\frac{\delta^2 k_n}{\delta\theta^2}\right|_{B_n=0}(\delta\theta)^2, \qquad (18)$$

$$\left.\frac{\delta^2 k_n}{\delta\theta^2}\right|_{B_n=0} = \frac{2\omega_I^2}{(\omega_{n+}\omega_{n-})^2}\left(\frac{\delta B_n}{\delta\theta}\right)^2 \approx 2\left(\frac{\delta B_n/\delta\theta}{\omega_I}\right)^2. \quad (19)$$

We find that $k_n B/(\delta\theta)^2 \sim 0.5\%$ T^2/deg^2. Thus, with a 1° error in the magnetic field direction and a field strength of 1 T, the sites that are not supposed to contribute to ESEEM when the field is oriented along [100] or [011] could, if occupied by a ^{29}Si nucleus, actually provide modulations up to about 1%. This, however, scales quadratically with the angle error, so an error of 1% of a degree would keep these errors below the 10^{-6} threshold often quoted for quantum error correction.

VII. CONCLUSION

We have studied Si:P donor electron spin decoherence due to AHF interaction, which is an important dephasing mechanism in Si. We clarify the electron spin echo envelope modulation in the Si:P system and the resonancelike contributions from nuclear spins in various shells away from the P atoms. Our theory is in excellent quantitative agreement with experiment. Most importantly, we suggest an approach to minimize the decoherence effect of AHF interaction by avoiding the cancellation conditions and orienting an applied magnetic field along directions that can periodically eliminate the contributions from the dominant E-shell nuclei. We quantitatively analyze the sensitivity of this strategy to errors in timing and magnetic field orientation.

In principle, one can eliminate the problem of nuclear spin decoherence through isotopic purification, removing the ^{29}Si. After purification, those donors that still have ^{29}Si nuclei in the E shell may be disqualified as qubits. Our strategy provides an alternative solution to this problem that provides the quantum computer architect with more flexibility.

[1] S. Das Sarma, R. de Souda, X. Hu, and B. Koiller, Solid State Commun. **133**, 737 (2004).

[2] R. Vrijen, E. Yablonovitch, K. Wang, H. W. Jiang, A. Balandin, V. Roychowdhury, T. Mor, and D. DiVincenzo, Phys. Rev. A **62**, 012306 (2000).

[3] M. Friesen, P. Rugheimer, D. E. Savage, M. G. Lagally, D. W. van der Weide, R. Joynt, and M. A. Eriksson, Phys. Rev. B **67**, 121301(R) (2003).

[4] B. E. Kane, Nature (London) **393**, 133 (1998).

[5] A. M. Tyryshkin and S. A. Lyon (private communication).

[6] A. Schweiger and G. Jeschke, *Principle of Pulse Electron Paramagnetic Resonance* (Oxford University Press, Oxford, 2001), Chaps. 8 and 10.

[7] E. B. Hale and R. L. Mieher, Phys. Rev. B **3**, 1955 (1971); J. L. Ivey and R. L. Mieher, *ibid.* **11**, 849 (1975).

[8] J.-M. Jancu, R. Scholz, F. Beltram, and F. Bassani, Phys. Rev. B **57**, 6493 (1998).

[9] B. Koiller, R. B. Capaz, X. Hu, and S. Das Sarma, Phys. Rev. B **70**, 115207 (2004).

[10] G. Feher, Phys. Rev. **114**, 1219 (1959).

[11] E. B. Hale and R. L. Mieher, Phys. Rev. **184**, 739 (1969).

[12] S. Saikin and L. Fedichkin, Phys. Rev. B **67**, 161302(R) (2003).

[13] W. B. Mims, Phys. Rev. B **5**, 2409 (1972).

[14] S. A. Dikanov and Y. D. Tsvetkov, *Electron Spin Echo Envelope Modulation (ESEEM) Spectroscopy* (CRC, Boca Raton, FL, 1992).

[15] A. M. Tyryshkin, S. A. Lyon, A. V. Astashkin, and A. M. Raitsimring, Phys. Rev. B **68**, 193207 (2003).

[16] A. M. Tyryshkin, J. J. L. Morton, S. C. Benjamin, A. Ardavan, G. A. D. Briggs, J. W. Ager, and S. A. Lyon, J. Phys.: Condens. Matter **18**, S783 (2006).

[17] E. Abe, K. M. Itoh, J. Isoya, and S. Yamasaki, Phys. Rev. B **70**, 033204 (2004).

[18] A. Ferretti, M. Fanciulli, A. Ponti, and A. Schweiger, Phys. Rev. B **72**, 235201 (2005).

[19] W. M. Witzel, Rogerio de Sousa, and S. Das Sarma, Phys. Rev. B **72**, 161306(R) (2005); W. M. Witzel and S. Das Sarma, *ibid.* **74**, 035322 (2006).

[20] E. J. Reijerse and S. A. Dikanov, J. Chem. Phys. **95**, 836 (1991).

[21] C. Kittel and A. H. Mitchell, Phys. Rev. **96**, 1488 (1954); J. M. Luttinger and W. Kohn, *ibid.* **97**, 869 (1955); W. Kohn and J. M. Luttinger, *ibid.* **98**, 915 (1955).

[22] W. Kohn, in *Solid State Physics*, edited by F. Seitz and D. Turnbull (Academic, New York, 1957), Vol. 5, p. 257.

[23] S. T. Pantelides, Rev. Mod. Phys. **50**, 797 (1978).

[24] Similar results are obtained if the Zeeman frequencies are randomly distributed by 0.4% instead of the HF frequencies, corresponding to a random field variation in the range of 10 G (or in some combination such that they combine in quadrature to 0.4%), though we believe that strain is more likely to affect HF interactions via small distortions in the electron wave function.

[25] Small strains can result even from mundane sources in an experiment. For example, in a private conversation, Y. Hirayama of the University of Tohoku pointed out that in a NMR experiment on a GaAs quantum point contact (Ref. 26), strain from the way the sample is mounted can result in a 15 kHz nuclear quadrupole splitting.

[26] G. Yusa, K. Muraki, K. Takashina, K. Hashimoto, and Y. Hirayama, Nature (London) **434**, 1001 (2005); G. Yusa, N. Kumada, K. Muraki, and Y. Hirayama, arXiv:cond-mat/0510310 (unpublished).

[27] H. Y. Carr and E. M. Purcell, Phys. Rev. **94**, 630 (1954); S. Meiboom and D. Gill, Rev. Sci. Instrum. **29**, 6881 (1958).

[28] W. M. Witzel and S. Das Sarma, Phys. Rev. Lett. **98**, 077601 (2007).

[29] K. Khodjasteh and D. A. Lidar, Phys. Rev. Lett. **95**, 180501 (2005).

[30] Wang Yao, Ren-Bao Liu, and L. J. Sham, Phys. Rev. Lett. **98**, 077602 (2007).